PROFESSOR SANG HUN LEE (Orcid ID : 0000-0002-6626-9702)

Article type : Original Manuscript

Melatonin protects chronic kidney disease mesenchymal stem cells against senescence via PrP^C dependent enhancement of the mitochondrial function

Yong-Seok Han[1] | SangMin Kim[1] | Jun Hee Lee[2] | Seo Kyung Jung[1] | Hyunjin Noh[3] | Sang Hun Lee[1,4]*

[1]Soonchunhyang Medical Science Research Institute, Soonchunhyang University, Soonchunhyang University Seoul Hospital, Seoul 04401, Republic of Korea

[2]Department of Pharmacology and Toxicology, University of Alabama at Birmingham School of Medicine, Birmingham, AL, U.S.A.

[3]Department of Internal Medicine, Soonchunhyang University, Seoul, Republic of Korea; Hyonam Kidney Laboratory, Soonchunhyang University, Seoul, Republic of Korea.

[4]Departments of Biochemistry, Soonchunhyang University College of Medicine, Cheonan 330-930, Korea

Running title: Melatonin inhibits CKD-MSC senescence by PrP^C

This article has been accepted for publication and undergone full peer review but has not been through the copyediting, typesetting, pagination and proofreading process, which may lead to differences between this version and the Version of Record. Please cite this article as doi: 10.1111/jpi.12535

***Correspondence:**

Sang Hun Lee, Soonchunhyang Medical Science Research Institute, Soonchunhyang University, Soonchunhyang University Seoul Hospital, 59 Daesagwan-ro (657 Hannam-dong), Yongsan-gu, Seoul 04401, Republic of Korea.

Tel: +82-02-709-9029; Fax: +82-02-792-5812; E-mail: ykckss1114@nate.com

Abstract

Although mesenchymal stem cell (MSC)-based therapy is a treatment strategy for ischemic diseases associated with chronic kidney disease (CKD), MSCs of CKD patients undergo accelerated senescence, with decreased viability and proliferation upon uremic toxin exposure, inhibiting their utility as a potent stem cell source for transplantation therapy. We investigated the effects of melatonin administration in protecting against cell senescence and decreased viability induced by pathophysiological conditions near the engraftment site. MSCs harvested from CKD mouse models were treated with H_2O_2 to induce oxidative stress. CKD-derived MSCs exhibited greater oxidative stress-induced senescence than normal-mMSCs, while melatonin protected CKD-mMSCs from H_2O_2 and associated excessive senescence. The latter was mediated by PrP^C-dependent mitochondrial functional enhancement; melatonin upregulated PrP^C, which bound PINK1, thus promoting mitochondrial dynamics and metabolism. *In vivo*, melatonin-treated CKD-mMSCs survived longer, with increased secretion of angiogenic cytokines in ischemic disease engraftment sites. CKD-mMSCs are more susceptible to H_2O_2-induced senescence than normal-mMSCs, and melatonin administration protects CKD-mMSCs from excessive senescence by up-regulating PrP^C and enhancing mitochondrial function. Melatonin showed favorable therapeutic effects by successfully protecting CKD-mMSCs from related ischemic conditions, thereby enhancing angiogenesis and survival. These results elucidate the

mechanism underlying senescence inhibition by melatonin in stem cell-based therapies using mouse-derived CKD-mMSCs.

KEYWORDS: chronic kidney disease, oxidative stress, cell senescence, melatonin, cellular prion protein

1 | INTRODUCTION

Chronic kidney disease (CKD) affects approximately 7.7% of the US population, gradually and persistently decreasing kidney function, which is detrimental to overall health.[1] CKD patients fail to emit toxic metabolites and organic waste solutes, which are normally eliminated via the healthy kidneys, with the accumulation of such toxins in these patients significantly increasing the risks of comorbidities including anemia, renal osteolytic disorder, neuropathy, and cardiovascular disease.[2-4] Despite the overbearing burden, currently available therapies against CKD often lead to adverse side effects and malignant pharmacokinetic changes. In response, the potential of mesenchymal stem cells (MSCs) and their clinical applicability against CKD have received increasing attention.[5-8] MSCs, adult stem cells capable of self-renewal and multipotent differentiation, constitute a promising cell source with strong regenerative and modulatory potentials for targeting numerous chronic diseases and complicated injuries. MSC transplantation therapy in animal models of various ischemic diseases, including kidney disease, have enhanced recovery and protection from further damage.[9]

However, one of the major drawbacks of MSC therapy is the exposure of MSCs harvested from CKD patients to endogenous uremic toxins that decrease their proliferative capacity and accelerate senescence, thereby decreasing the therapeutic potential.[10,11] Cells

within these patients reportedly exhibit dysfunctional mitochondrial-related intracellular machinery and disrupted mitochondrial homeostasis, rendering CKD-derived MSCs more prone to pathological damage.[12,13] Clinically, transplantation efficiency of MSCs is less than 10%, owing to these pathophysiological conditions, including oxidative stress and inflammation associated with the engraftment site of the transplanted cells.[14] Moreover, following transplantation, MSCs harvested from CKD model mice showed decreased proliferation and secretion of the modulatory angiogenic cytokines facilitating neovascularization.[15] Accordingly, CKD-MSC transplantation *in vivo* in ischemic models did not significantly increase the transplantation efficacy or rescue neovascularization.[16] Therefore, to increase the applicability of stem cell transplantation therapy in patients with CKD, novel approaches are needed to overcome the pathologic conditions of CKD-MSCs to resist detrimental environmental stress induced by the engraftment site.

Furthermore, CKD patients experience various sleeping disorders, suggesting a potential association between CKD and sleep and with the regulation of the endogenous sleep-regulating hormone melatonin.[17] Melatonin, a pineal gland secretion associated with sleep induction, regulates circadian rhythms and homeostasis.[18-20] Melatonin reportedly supplements MSC viability and applicability by increasing MSC motility and proliferation, thereby enhancing the therapeutic effect of MSC transplantation.[21] Previously, we suggested that melatonin protects against p-cresol (a uremic toxin in CKD patients)-induced stem cell senescence.[22] Furthermore, melatonin-treated stem cell-based therapies have significant therapeutic effects on ischemic diseases, demonstrating its potential as a supplemental drug to enhance autologous MSC transplantation in CKD patients, offering a potent therapeutic strategy to alleviate the deleterious cardiovascular disease associated with CKD.[23-25]

Herein, we aimed to evaluate the therapeutic effects of melatonin on autologous CKD-MSCs subjected to H_2O_2-induced senescence. In addition, we sought to delineate the mechanisms by which melatonin rescues senescence and CKD-MSC deterioration from oxidative stress via examination of the PrP^C-mitochondrial pathway. Finally, we assessed the applicability of enhanced stem cell transplantation in an *in vivo* ischemic model to delineate the clinical applicability of melatonin-enhanced CKD-MSC transplantation therapy.

2 | MATERIALS AND METHODS

2.1 | Isolation of bone marrow-derived MSCs from a CKD mouse model

A murine CKD model was established in BALB/c nude mice (8 to 10 weeks old). The mice underwent electrocoagulation of the left kidney surface with a small portion of the hilum intact, and after 2 weeks, the mice underwent surgical ablation of the contralateral right kidney. All experiments were randomized and blinded. Bone marrow-derived MSCs were harvested from the hind limb long bone.[26] Isolated bone marrow was centrifuged and suspended in primary culture medium, and bone marrow-derived MSCs were cultured in a humidified incubator at 37°C and 95% air and 5% CO_2. Normal and CKD MSCs cell lines were separated from each group by 5 mice. All MSCs were characterized for each cell line (Supplemental Figure 1). All experimental replicates were performed using normal- or CKD-mouse MSCs (mMSC) derived from different mouse donors.

2.2 | β-galactosidase staining assay

Senescence was assessed by measuring the number of cultured cells staining positive for the senescence-associated β-galactosidase (SA-β-gal). Cells were washed twice with phosphate-buffered saline (PBS), fixed with 2% formaldehyde/0.2% glutaraldehyde (Sigma-Aldrich, St. Louis, MO, USA), and incubated at 37°C (without CO_2) for 12 h with a β-gal staining

solution (1 mg/mL X-Gal, 40 mM citric acid-sodium phosphate buffer, 150 mM NaCl, 2 mM $MgCl_2$, 5 mM potassium ferrocyanide, and 5 mM potassium ferricyanide; pH 6.0; Sigma-Aldrich). Stained (blue, positive) and unstained (negative) cells were enumerated via phase-contrast microscopy (Nikon, Tokyo, Japan) in five independent cultures. Experiments were performed in triplicate.

2.3 | Western blot analysis

Total cellular proteins (20 μg protein) were separated using 10% sodium dodecyl sulfate-polyacrylamide gels. Separated proteins were electro-transferred to a nitrocellulose membrane. After washing with TBST (10 mM Tris-HCl [pH 7.6], 150 mM NaCl, and 0.05% Tween-20), the membranes were blocked with 5% skim milk for 2 h and then incubated with the following primary antibodies: anti-p-P53, anti-P16INK4A, anti-SMP30, anti-P21, anti-PrP^C, anti-PINK, anti-phospho-DRP-1 (S637), anti-OPA-1, anti-CDK2, anti-CDK4, anti-Cyclin E, anti-Cyclin D1, and anti-β-actin antibodies (Santa Cruz Biotechnology, Dallas, TX, USA). After incubating the membranes with primary antibodies, peroxidase-conjugated secondary antibodies (Santa Cruz Biotechnology) were applied. Protein bands were detected using enhanced chemiluminescence (ECL) reagents (Amersham Biosciences, Little Chalfont, UK) in a dark room. Experiments were performed in triplicate.

2.4 | Mitochondrial Morphology

Mitochondria in mMSCs was stained using Mito-Tracker red (Life Technologies, Carlsbad, CA, USA). Cells were cultivated on a cover slip and Mito-Tracker was added to growth media at a concentration of 25 nM for 30 min at 37°C. Cells were fixed with 4% formaldehyde for 30 min. The nucleus was stained using 4′,6-diaminido-2-phenylindol (Vector Laboratories, Burlingame, CA, USA) and images were taken using the ZEISS LSM 880 microscope.

2.5 | Isolation of Mitochondrial Fractions

Cells were placed in 1 ml isolation buffer (215 mM mannitol, 75 mM sucrose, 0.1% bovine serum albumin, 20 mM HEPES; pH 7.2) with 1 mM EGTA. On adding the protease inhibitor, the mixture was centrifuged at 5000 ×g for 20 min at 4°C. The pellet contained the mitochondrial fraction and was resuspended in isolation buffer; isolated mitochondria were stored at 4°C.

2.6 | siRNA transfection

Lipofectamine 2000 reagent (Thermo Fisher Scientific, Rockford, IL, USA) and PRNP-specific SMART pool siRNAs (100 nM) (Dharmacon, Lafayette, CO, USA) were mixed and incubated for 15 min at room temperature. MSCs were cultured to 70% confluence in culture medium, which was then changed to medium not containing FBS and antibiotic regents. The mixture was treated with MSCs and cultured for 48 h at 37°C. Transfected MSCs were used in experiments after replacing the medium with siRNA-free growth medium.

2.7 | Co-immunoprecipitation

We disrupted normal-mMSCs and CKD-mMSC via sonication in a co-immunoprecipitation buffer. PINK1-PrP^C complexes were precipitated for 4 h at 4°C, using an anti-PINK1 antibody-conjugated agarose bead (Santa Cruz Biotechnology). Subsequently, PBS washing was performed twice and 500 ug of cell lysate in the protein bead was incubated overnight at 4°C. PrP^C was detected using anti-PrP^C antibodies (Santa Cruz Biotechnology) via western blot analysis. The product was reduced with sodium borohydrid, and the absorbance was measured at 550 nm.

2.8 | Complex I and IV activity

The submitochondrial fractions (0.6 mg/mL) were incubated for 3 min in a medium (250 mM sucrose, 50 mM potassium-phosphate, 1 mM KCN, 50 lM decylubiquinone, 0.8 lM antimycin, pH 7.4). Complex I activity was measured from the rate of the oxidation of NADH (100 mm) at 340 nm. Complex IV activity was measured by adding 75 ml of cytochrome c previously reduced with sodium morohydrid and determining the absorbance at 550 nm.

2.9 | Measurement of extracellular oxygen consumption rate

We measured the extracellular oxygen uptake (OCR) of cells using the Extracellular O_2 Consumption Assay Kit (cat # ab197243, Abcam, USA). Normal- or CKD-mMSCs with or without *si-PRNP* or *siScr* (5 * 10^3 cells / well in 150 uL culture media) were plated on 96 well cell culture plates, and incubated in a CO_2 incubator at 37 °C overnight. The culture medium was removed and replaced with 150 µL of fresh culture medium supplemented with Melatonin (100 µM), and incubated in a CO_2 incubator at 37 °C for 30 min. And, add H_2O_2 (25 µM), and incubated in a CO_2 incubator at 37 ° C for 72 h. A 10 µL of Extracellular O_2 Consumption reagent and two drops of pre-warmed High Sensitivity mineral oil were added to each well and measured using a multi-detection microplate reader (Victor3, Perkin Elmer, USA). Extracellular O_2 Consumption was measured at 37 °C for 80 minutes at 2 minute intervals using wavelengths of 340 and 650 nm.

2.10 | Assessment of Growth factors

Vascular endothelial growth factor (VEGF), fibroblast growth factor (FGF), and hepatocyte growth factor (HGF) levels in the normal and CKD-mMSC lysates or ischemic limb tissue lysates 3 d after cell transplantation were determined via ELISA using a commercially available ELISA kit (R&D Systems, Minneapolis, MN, USA) per the manufacturer's

recommendation. Protein quantification was performed using bicinchoninic acid assay and absorbance was measured at 450 nm, using a microplate reader (Tecan Group AG, Männedorf, Switzerland).

2.11 | Inflammatory cytokine assay

Ischemic tissue was harvested to determine interleukin (IL)-10 and tumor necrosis factor (TNF)-α levels, using respective ELISA kits (Koma Biotechnology, Seoul, Korea) per the manufacturer's instructions. TNF-α and IL-10 levels in the standard solutions and samples were quantified by measuring the absorbance at 450 nm, using a microplate reader (Tecan).

2.12 | Adhesion assay

After coating 48-well culture plates with collagen 1, cells were trypsinized and cultured on collagen 1-coated culture plates for 1 h. The cells were then washed twice with PBS and stained with Crystal Violet. The dye staining the cells was extracted with 10% acetic acid and measured at OD_{560}, using a microplate reader (BMG labtech, Ortenberg, Germany).

2.13 | Single-cell cultivation assay

MSCs in culture were dissociated into a single-cell suspension using trypsin, and their density was adjusted to 1 cell per 100 μL via a limited-dilution assay. Suspend MSCs were seeded in 96-well plates at 100 μL per well, and cultured (at one cell per well). After 12 h, MSCs adhered to the plate were treated with melatonin. MSCs were cultured in an incubator with 5% CO_2 at 37°C for 10 d. Experiments were performed in triplicate.

2.14 | Cell cycle analysis

Normal-mMSCs and CKD-mMSCs treated with H_2O_2, melatonin, and *PRNP* siRNA were fixed using 70 % ethanol at −20 °C for 24 h. Cells were incubated with RNase and propidium iodide (PI) for cell cycle analysis (SysmexPartec GmbH, Gorlitz, Germany). Cell cycle distribution was assessed using a FACS analysis (Cyflow Cube 8, Partec, Munster, Germany). Data analysis was performed using standard FSC Express (De Novo Software, Los Angeles, CA, USA).

2.15 | Carboxyfluorescein succinimidyl ester (CFSE) staining assay

CFSE was used to assess MSC proliferation, as analytical measurements have shown that CFSE positivity decreases upon enhancing proliferation but increases when cell proliferation is suppressed. MSCs were washed once in PBS and diluted in 1 mL of modified Eagle's medium alpha supplemented with 5% fetal bovine serum, then stained with 10 μM CFSE (Molecular Probes, Eugene, OR, USA) for 10 min at room temperature in the dark during staining. Subsequently, cells were washed thrice with PBS and stained MSCs were cultured at 5% CO_2 at 37°C. After H_2O_2 and melatonin treatment, CFSE staining was performed and the sample was analyzed using the green (FL1) channel of a flow cytometer (Sysmex partec, Görlitz, Germany). Experiments were performed in triplicate.

2.16 | GFP cell labeling

The pGFP-C-shLenti vector (OriGene Technologies, Rockville, MD, USA) was used to transfect normal and CKD-mMSCs. The cells were then incubated in growth medium supplemented with puromycin (2 μg/ml) for 14 d. Thereafter, resistant cells were specifically selected, and each individual cell was incubated in growth media without puromycin.

2.17 | Murine hind limb ischemia model

The murine hind limb ischemia model was established as previously described, with minor modifications.[27] Ischemia was induced by ligation and excision of the proximal femoral artery and boundary vessels of the mice. No later than 6 h after surgery, MSCs were injected intramuscularly into the ischemic thigh (5×10^5 cells/100 μL PBS per mouse; 5 mice per treatment group) in sham-operated or CKD mice (an acute murine hind limb ischemia model). Cells were injected into multiple (five) ischemic sites. Blood perfusion was assessed from the ratio of blood flow in the ischemic (left) limb to that in the non-ischemic (right) limb on postoperative days 0, 3, 7, 14, 21, and 28, using laser Doppler perfusion imaging (LDPI; Moor Instruments, Wilmington, DE, USA).

2.18 | Immunohistochemistry

The ischemic thigh areas were dissected after 3 or 28 d post-MSC transplantation, fixed with 4% paraformaldehyde (Affymetrix, Santa Clara, CA, USA), and embedded in paraffin. For histological analysis, slides were stained with hematoxylin and eosin (H&E) and Sirius red. The range of necrosis and collagen fibrosis area was quantified as a percentage using Image J software. Immunofluorescence was performed using primary antibodies against TNF-α, IL-10, proliferating cell nuclear antigen (PCNA), cleaved-caspase3, Ki67, anti-mouse/human alpha-smooth muscle actin (α-SMA), and anti-mouse/human CD31 (Santa Cruz Biotechnology), followed by secondary antibodies conjugated with Alexa488 and Alexa594 (Life Technologies, Carlsbad, CA, USA). Nuclei were stained with 4′,6-diaminido-2-phenylindol (Vector Laboratories, Burlingame, CA, USA). Images were acquired via confocal microscopy (Olympus, Tokyo, Japan).

2.19 | Terminal deoxynucleotidyl transferase-mediated dUTP nick-end labeling (TUNEL) assay

We used a TdT fluorescein in situ apoptosis detection kit (Trevigen Inc, Gaithersburg, MD, USA). The TUNEL assay was performed for ischemic tissue at day 3 post surgery. Stained sections were visualized using a confocal microscope (Olympus).

2.20 | Statistical analysis

Results are expressed as the means ± standard error of the mean (SEM). All experiments were analyzed using one-way analysis of variance, followed by Bonferroni–Dunn test for post hoc analysis. Differences were considered statistically significant if $P < 0.05$.

3. RESULTS

3.1 | CKD-mMSCs show greater cell senescence upon oxidative stress

We isolated normal-mouse(m)MSCs and CKD-mMSCs and evaluated their differentiation potential. The characteristics of normal-mMSCs and CKD-mMSCs were not significantly different (Supple Fig. 1). MSCs harvested from normal and CKD mouse models were treated with low concentrations of H_2O_2 (25 uM; Supple Fig. 2) followed by β-galactosidase staining to confirm accelerated cell senescence by H_2O_2 of CKD-mMSCs. CKD-mMSCs yielded a greater number of β-gal-positive cells in 25 μM H_2O_2 than did normal-mMSCs (Fig. 1A and 1B). In addition, CKD-mMSCs were larger than normal-mMSCs upon treatment with H_2O_2 (Fig. 1C and 1D). We further conducted molecular assays to confirm the promotion of cellular senescence of CKD-mMSCs by H_2O_2. Low H_2O_2 concentrations upregulated p-P53 and p16INK4A in CKD-mMSCs than in normal MSCs (Fig. 1E and 1F). SMP30, a marker of cellular senescence, was significantly downregulated upon treatment of CKD-mMSCs with 25 μM H_2O_2 (Fig. 1F), whereas P21 was upregulated (Fig. 1H). These results demonstrate that CKD-mMSCs exhibit cellular senescence at a very low concentration (25 μM) of H_2O_2.

3.2 | Melatonin alleviates oxidative stress-induced cellular senescence

To confirm the effect of melatonin on the cell senescence of CKD-mMSCs from H_2O_2, MSCs were pretreated with melatonin followed by treatment with H_2O_2. Melatonin pretreatment restored cellular morphology of H_2O_2-enlarged cells, with 100 μM melatonin most effectively reducing cell size (Fig. 2A and 2B). In addition, 100 μM melatonin-treated CKD-mMSCs showed a substantial reduction in the number of β-gal-positive cells (Fig. 2C and 2D). Furthermore, melatonin significantly downregulated p-P53 and p16INK4A (Fig. 2E and 2F), upregulated SMP30 reduced by H_2O_2, and significantly downregulated P21 (Fig. 2G and 2H). These results demonstrated that while CKD-mMSCs respond more sensitively to H_2O_2 than normal-mMSCs and are more likely to exhibit cell senescence, melatonin induces CKD-mMSCs to protects against H_2O_2-induced senescence. Therefore, our findings indicated that melatonin protects CKD-derived MSCs from H_2O_2, thereby facilitating cell proliferation and adhesion.

3.3 | Protective effects of melatonin on cell senescence through the regulation of PrP^C expression

We quantified PrP^C expression in cells to determine how melatonin protected CKD-MCSs from senescence. CKD-MCSs treated with H_2O_2 exhibited decreased PrP^C, whereas melatonin pretreatment significantly upregulated PrP^C (Fig. 3A). We also used PrP^C-specific siRNAs to confirm the involvement of PrP^C in melatonin-mediated protection against cellular senescence. CKD-mMSCs with siRNA-mediated knockdown of PrP^C did not protect against the reduction in SMP30 by H_2O_2 after treatment with melatonin and did not decrease the H_2O_2-induced upregulation of p-P53, p16INK4A, and P21 (Fig. 3B-3E). Moreover, the suppression of PrP^C in normal-mMSCs rendered these cells susceptible to downregulation of SMP30 and upregulation of p-P53, p16INK4A, and P21 by H_2O_2 (Fig. 3F-3I). In addition,

the number of β-gal-positive cells in normal-mMSCs was most abundant upon suppression of PrP^C expression (Fig. 3J and 3K). Furthermore, overexpression of PrP^C in CKD-mMSC protected against oxidative stress-induced senescence (Supple Fig. 3). Hence, PrP^C expression is associated with MSC senescence and melatonin suppresses cell senescence by regulating PrP^C expression in CKD-mMSCs.

3.4 | Melatonin enhances mitochondrial activity via PrP^C expression in CKD-mMSCs

To confirm that melatonin helps retain mitochondrial function via PrP^C expression, we first demonstrated that PrP^C binds to PINK1 in mitochondria in normal-mMSCs, with reduced binding in CKD-mMSCs. Melatonin treatment increased the binding of PrP^C and PINK1 in the mitochondria of CKD-mMSCs (Fig. 4A). These results suggest that PINK1 in mitochondria bound to PrP^C may increase mitochondrial dynamics and protect against senescence. Furthermore, PINK1 was regulated via PrP^C expression in melatonin-treated cells (Fig. 4B). In addition, melatonin pretreatment downregulated phosphorylated (p) S637-Drp-1, the inactive state of a mitochondrial fission-associated protein, an effect that was alleviated via siRNA-mediated knockdown of PrP^C in CKD-mMSCs (Fig. 4C), and downregulated H_2O_2-enhanced Mfn1 and OPA-1 associated with mitochondrial fusion (Fig. 4D and 4E). In addition, to confirm the mitochondrial morphology, staining with Mito-Tracker was performed. Mitochondrial fusion in CKD-mMSCs increased on exposure H_2O_2, but exposure to melatonin increased mitochondrial fission. However, the silencing of PrP^C did not facilitate melatonin-induced mitochondrial fission (Fig. 4F). These results indicated that melatonin pretreatment upregulated PrP^C and increased mitochondrial remodeling. Moreover, melatonin pretreatment restored H_2O_2-reduced activity of mitochondrial complexes I and IV, which was dependent on PrP^C expression. However, when PrP^C was inhibited, the activity of complex I and IV decreased again (Fig. 4G and 4H). In addition,

melatonin inhibited H_2O_2-induced reductions in oxygen consumption in CKD-mMSCs (Fig. 4I). Moreover, overexpression of PrP^C in CKD-mMSC increased the activity of complexes I and IV, thereby augmenting mitochondrial oxidative phosphorylation (Supple Fig. 4A-4C). Hence, melatonin upregulated PINK1 via regulation of PrP^C, thereby enhancing mitochondrial dynamics and function.

3.5 | Effect of melatonin on the recovery of MSC function via PrP^C regulation

Along with inhibition of H_2O_2-mediated cell senescence in CKD-mMSCs, melatonin is involved in the restoration of cell proliferation. Melatonin pretreatment upregulated CDK2, CyclinE, CDK4, and Cyclin D1, which comprise cell proliferation-related proteins that are downregulated by H_2O_2, whereas inhibition of PrP^C expression precluded this effect (Fig. 5A and 5B). In addition, cell proliferation, as determined by CFSE staining, was retained upon melatonin pretreatment in CDK-MSCs with H_2O_2-reduced proliferation in a PrP^C-dependent manner (Fig. 5C and 5D). Furthermore, the S phase in CDK-mMSCs was also restored by the increase in the level of melatonin-induced PrP^C (Fig. 5E and 5F), with similar results obtained in the single-cell assay (Fig. 5G and 5H). These findings suggest that melatonin regulates PrP^C to support proliferation of CKD-mMSCs. Furthermore, modulation of PrP^C expression by melatonin is required to increase the cell attachment capacity of CKD-mMSCs following H_2O_2 exposure (Fig. 5I and 5J). Similarly, PrP^C overexpression in CKD-mMSCs increased cell proliferation and adhesion (Supple Fig. 4D and 4E). In addition, melatonin upregulated angiogenic cytokines including VEGF, FGF, and HGF in CKD-mMSCs (Fig. 5K). Hence, melatonin is involved not only in the cellular senescence of CKD-mMSCs but also in their cell proliferation and secretion of angiogenic cytokines.

3.6 | Melatonin-mediated increase in PrP^C levels enhances MSC survival at the ischemic site

To investigate whether the transplanted melatonin-pretreated GFP-transfected CKD-mMSCs exhibited increased survival at the ischemic site via PrP^C expression, ischemic tissues were harvested on postoperative day 3 and subjected to assessment of inflammatory cytokines and immunofluorescence staining. Melatonin-treated CKD-mMSCs had upregulated IL-10, an anti-inflammatory cytokine, and downregulated TNF-alpha, a pro-inflammatory cytokine (Fig. 6A-D). The expression of cleaved caspase-3 was significantly decreased in tissue injected with melatonin-pretreated GFP-positive CKD-mMSCs, compared to other groups (Fig. 6E and 6F). TUNEL staining also showed the significant reduction of apoptosis in tissues injected with melatonin-pretreated CKD-mMSCs (Fig. 6G and 6H). However, this effect was inhibited upon pretreatment of CKD-mMSCs with the *PRNP* siRNA (Fig. 6E-6H). In addition, cell proliferation increased in tissue transplanted with melatonin-pretreated GFP-positive CKD-mMSCs; however, in cells with PrP^C inhibition, the proliferating cell numbers decreased (Fig. 6I-6L). Furthermore, PrP^C overexpression in CKD-mMSCs also yielded similar effects (Supple Fig. 4F-4I). Hence, melatonin increases proliferation by increasing the survival rate of transplanted CKD-mMSCs.

3.7 | Melatonin enhances neovascularization via PrP^C expression in ischemic tissue

To determine whether neovascularization occurred following the enhancement of vascular repair upon transplantation of melatonin-pretreated CKD-mMSCs *in vivo*, angiogenic cytokine expression, blood perfusion, and tissue repair were assessed. On day 3 after cell transplantation, the secretion of angiogenic cytokines (VEGF, FGF, and HGF) was significantly increased at the ischemic site (Fig. 7A). On day 28 after cell transplantation, CKD-MSCs elicited lesser vascular repair than normal-mMSCs. However, the melatonin-

treated CKD-mMSC group exhibited significantly increased blood flow compared to that in the CKD-mMSC group, although the therapeutic effect of melatonin treatment was precluded upon inhibition of PrP^C expression (Fig. 7B and 7C). Similarly, transplantation of melatonin-treated CKD-mMSCs salvaged the entire mouse paw, whereas the group with inhibited PrP^C expression developed necrosis even in the presence of melatonin (Fig. 7D). Furthermore, to evaluate the effects of melatonin pretreatment of MSCs on neovascularization, we performed immunofluorescence staining for CD31 (capillary marker) and αSMA (arteriole marker) within the ischemic tissues of mice in each group on postoperative day 28 (Fig. 7E-7H). The melatonin-treated CKD-mMSC group exhibited greater blood vessel density than the other groups. In addition, transplantation of melatonin-pretreated CKD-mMSCs inhibited necrosis in the ischemic area and reduced the formation of collagen fibers (Fig. 7I-L). Hence, melatonin-treated CKD-mMSCs promote angiogenesis via expression of PrP^C in ischemic tissues.

4. DISCUSSION

This study aimed to elucidate the precise mechanism by which melatonin inhibits H_2O_2-induced CKD-mMSC senescence via PrP^C-induced mitochondrial dynamics. CKD-mMSCs are more susceptible than normal-mMSCs to H_2O_2-induced senescence, and the preemptive administration of melatonin protects the CKD-mMSCs from excessive senescence via PrP^C upregulation and enhanced mitochondrial function. In addition, melatonin successfully protects CKD-mMSCs from the detrimental effects related to ischemic conditions *in vivo*, thereby increasing angiogenesis and survival of the injury.

MSC transplantation has gained significant interest as a therapeutic intervention for patients with CKD-associated cardiovascular diseases. In particular, autologous MSC transplantation therapy using a patient's own MSCs is preferred over allogenic therapy to

overcome the immune rejection of transplanted MSCs.[28] However, the therapeutic feasibility of autologous MSC transplantation among CKD patients is significantly attenuated by uremic toxins that deteriorate endogenous MSC viability and functionality.[26] This study investigated whether CKD-mMSCs have greater susceptibility toward oxidative conditions *in vitro*, similar to conditions at the recipient engraftment ischemic site. We found that MSCs from a CKD mouse model experience increased senescence under externally induced H_2O_2 compared normal-mMSCs. In particular, treatment of CKD-mMSCs with relatively low concentrations of H_2O_2 (5–25 μM) induced greater positive staining of SA-β-gal activity, increased cell size, downregulated SMP30, and upregulated P21 at 25 μM H_2O_2 than that in normal-mMSCs, suggesting that the CKD-mMSCs are more susceptible to H_2O_2 and progression to cell senescence compared to the control. These results suggest a supplementary approach to potentiate weakened CKD-mMSCs to withstand pathophysiological conditions occurring during clinical transplantation.

We previously reported that melatonin enhances MSC viability and motility, stemness, and proliferation and inhibits senescence induced by uremic toxins accumulated in CKD, thereby inducing the proliferation of MSC.[21,29] In addition, melatonin treatment of MSCs also effectively allows cells to withstand the pathophysiological conditions of the environment near the ischemic engraftment site[23-25] via precise mechanisms such as the induction of antioxidant enzymes and pro-angiogenic cytokines.[30] In the present study, we hypothesized that melatonin serves as a potent supplemental drug to rescue the CKD-mMSCs from the increased senescence and damage consequent to H_2O_2. Similar to the effects in normal cells, our results showed that melatonin inhibits the accelerated cell senescence observed in the CKD-mMSCs following treatment with 25 μM H_2O_2. Specifically, pretreatment with 100 μM melatonin inhibited cell senescence markers including positive staining of SA-β-gal activity, reduced cell size, upregulated SMP30 protein, and downregulated P21 protein via H_2O_2.

PrP^C, expressed ubiquitously, is critical for MSC viability and survival and is closely associated with senescence.[31] Owing to increasing reports, we aimed to determine whether PrP^C expression is relatively lower in CKD-mMSCs than in normal-mMSCs, and whether PrP^C expression plays an important role in CKD-mMSC viability against oxidative stress. Our results demonstrated that CKD-mMSCs had downregulated PrP^C compared to normal-mMSCs, suggesting that PrP^C downregulation may be directly associated with increased susceptibility. Furthermore, we observed that inhibition of PrP^C expression by *PRNP* siRNA nullified the protective effects of melatonin against the senescence induced by H_2O_2 in the CKD-mMSCs. Specifically, our results showed that SMP30 was downregulated, whereas P21 was upregulated, and that positive staining of SA-β-gal activity was increased when PrP^C expression was knocked down via si*PRNP*. Our findings thus suggest that melatonin protects against senescence induced by H_2O_2 in CKD-mMSCs in a PrP^C-dependent manner. Despite existing studies on melatonin treatment of MSCs, including our own, which provide evidence for the potential applicability of melatonin-treated MSC transplantation for targeting CKD, the precise mechanism underlying the protection of CKD-mMSCs against senescence by melatonin is unclear. Recent studies have reported that melatonin prevents oxidative stress via regulation of sirtuin 1 (SIRT1) and 3.[32-34] Melatonin upregulates SIRT1 and SIRT3, which increase antioxidant enzyme levels, superoxide dismutase, thereby protecting against oxidative stress-induced apoptosis.[32-34] Furthermore, knockdown of SIRT1 downregulated the prion protein.[35] We previously reported that melatonin increases stem cell proliferation and prevents apoptosis induced by oxidative stress via a PrP^C-dependent pathway.[27] These findings suggest that the melatonin-mediated protective effect of PrP^C on oxidative stress might be regulated by the SIRT family; however, the detailed correlation between PrP^C and SIRT family is needed to be investigated.

Mitochondria are essential cell organelles that play an important role in cell homeostasis.[36,37] Mitochondrial dysfunction induced by oxidative stress is directly related to stem cell senescence and reduced cellular function.[38] Specifically, Lee et al. reported that mitochondrial fusion may represent a major mechanism underlying senescence-related cellular dysfunction,[39] and Chandana et al. reported that PINK1 increases mitochondrial activation.[40] Herein, administration of melatonin to CKD-mMSCs increased the binding of PrP^C and PINK1 in the mitochondria. In addition, the level of PINK1 in the mitochondria increased, whereas that of p-Drp1, and Mfn-1 and OPA-1, associated with inactive mitochondrial fission and of mitochondrial fusion, respectively, decreased. In addition, mitochondrial complexes I and IV increased. Furthermore, expression of *PRNP*, encoding PrP^C protein, increased mitochondrial fusion and oxidative stress.[41] Concurrently, we found that inhibition of PrP^C expression by *PRNP* siRNA in the CKD-mMSCs increased Drp1 phosphorylation and decreased complex I and IV activity in the mitochondria despite melatonin treatment. Our results therefore delineate that mitochondrial regulation involves a pathway, wherein melatonin protects CKD-mMSCs through the up-regulation of PrP^C.

Mitochondrial dynamics and regulation are precisely associated with not only cellular senescence but also with the overall function and fate of the cell, including both proliferation and ultimate survival. We therefore evaluated the protective effect of melatonin via regulation of PrP^C toward the proliferation and survival of CKD-mMSCs exposed to H_2O_2. We found that melatonin markedly upregulated cell cycle activators, which were downregulated by H_2O_2 in CKD-mMSCs. Furthermore, the adhesiveness of CKD-mMSCs was restored in a PrP^C-dependent manner. Therefore, our results suggested that melatonin protects against H_2O_2-induced senescence along with decreased proliferation and survival via PrP^C-dependent protection of mitochondrial function, ultimately enhancing the proliferation and adhesion of treated CKD-mMSCs.

In addition, melatonin also protects adipose-derived MSCs from oxidative stress in myocardial infarction through induction of antioxidant enzymes and proangiogenic cytokines.[32] Therefore, we investigated the role of the melatonin-PrP^C pathway in the cytoprotective effects of melatonin and the therapeutic effect on ischemic disease during CKD-mMSC-based therapy. We found that melatonin-treated CKD-mMSCs transplanted into a hind limb ischemic area decreased apoptosis and increased cell proliferation, whereas when PrP^C expression was inhibited, while apoptosis and proliferation decreased. Thus, melatonin could increase engraftment via PrP^C expression in CKD-mMSCs. In addition, melatonin-treated CKD-mMSCs transplanted into the ischemic site significantly increased angiogenesis and blood flow, thus enhancing its therapeutic effect on ischemic disease. However, angiogenesis and blood flow were not restored in CKD-mMSCs with inhibited PrP^C expression despite treatment with melatonin.

A murine hind limb ischemia model is essentially an acute ischemic limb model which characterized by sudden reduction of blood perfusion of the limb, thereby threatening limb viability.[42,43] In chronic ischemia, collateral blood vessels may compensate blood perfusion when arteries are occluded, whereas acute ischemia induced limb necrosis because of limited time for angiogenesis. Therefore, several studies involved the injection of stem/progenitor cells in a murine hind limb ischemic tissues within 0 to 24 h.[44,45] A recent study reported that injection of human embryonic stem cell-derived endothelial cells increased the ratio of blood perfusion in an established ischemia model (transplantation of cells on post-operation day 3).[45] However, capillary formation did not increase significantly upon injection of cells in the established ischemia model; however, it increased significantly upon injection of cells in the acute ischemia model (transplantation of cells after limb ischemia operation).[45] These results indicate that early injection of cell-based therapeutic agents is important for patients with acute limb ischemia. However, further investigation is warranted to determine the timing of

transplantation of stem/progenitor cell-based therapeutics in an acute and chronic limb ischemia model for application in clinical trials.

In conclusion, we confirmed that CKD-mMSCs are more sensitive than normal-mMSCs to H_2O_2 and progression to cell senescence. H_2O_2-mediated senescence resulted from decreased mitochondrial activity because of increased mitochondrial fusion consequent to the low PrP^C expression of CKD-mMSCs. However, melatonin upregulated PrP^C in CKD-mMSCs and promoted mitochondrial fission, resulting in mitochondrial activity, thereby inhibiting senescence upon H_2O_2 treatment. In particular, transplantation of melatonin-treated CKD-mMSCs into an animal model of ischemic disease exhibited a highly therapeutic effect (Fig. 8). Moreover, to investigate the possibility for clinical trials, the present results verified the protective effects of melatonin in human MSCs harvested from CKD patients, against oxidative stress (Supple Fig. 5). Therefore, this study suggests that the mechanism underlying the inhibition of senescence by melatonin in stem cell-based therapies using MSCs derived from CKD patients might depend on enhancements in mitochondrial functional activity through regulation of PrP^C expression.

ACKNOWLEDGEMENTS

This study was supported by a National Research Foundation grant funded by the Korean government (NRF-2017M3A9B4032528). The funders had no role in the study design, data collection or analysis, the decision to publish, or preparation of the manuscript.

CONFLICT OF INTEREST

The authors declare no conflicts of interest.

AUTHOR CONTRIBUTIONS

Y.S.H. contributed to acquisition of data, analysis and interpretation of data, and drafting of the manuscript. S.M.K, J.H.L and S.K.J. interpreted the data, performed statistical analysis, and drafted the manuscript. H.J.N. contributed to the modification of the revised manuscript. S.H.L. developed the study concept and design, acquired, analyzed, and interpreted the data, drafted the manuscript, procured funding, and supervised the study.

REFERENCES

1. Castro AF, Coresh J. CKD surveillance using laboratory data from the population-based National Health and Nutrition Examination Survey (NHANES). *Am J Kidney Dis.* 2009;53(3 Suppl 3):S46-55.
2. D'Hooge R, Van de Vijver G, Van Bogaert PP, Marescau B, Vanholder R, De Deyn PP. Involvement of voltage- and ligand-gated Ca2+ channels in the neuroexcitatory and synergistic effects of putative uremic neurotoxins. *Kidney Int.* 2003;63(5):1764-1775.
3. Meijers BK, Claes K, Bammens B, et al. p-Cresol and cardiovascular risk in mild-to-moderate kidney disease. *Clin J Am Soc Nephrol.* 2010;5(7):1182-1189.
4. Gabriele S, Sacco R, Altieri L, et al. Slow intestinal transit contributes to elevate urinary p-cresol level in Italian autistic children. *Autism Res.* 2016;9(7):752-759.
5. Choi S, Park M, Kim J, Hwang S, Park S, Lee Y. The role of mesenchymal stem cells in the functional improvement of chronic renal failure. *Stem Cells Dev.* 2009;18(3):521-529.

6. Cavaglieri RC, Martini D, Sogayar MC, Noronha IL. Mesenchymal stem cells delivered at the subcapsule of the kidney ameliorate renal disease in the rat remnant kidney model. *Transplant Proc.* 2009;41(3):947-951.

7. Lee SR, Lee SH, Moon JY, et al. Repeated administration of bone marrow-derived mesenchymal stem cells improved the protective effects on a remnant kidney model. *Ren Fail.* 2010;32(7):840-848.

8. Li B, Morioka T, Uchiyama M, Oite T. Bone marrow cell infusion ameliorates progressive glomerulosclerosis in an experimental rat model. *Kidney Int.* 2006;69(2):323-330.

9. Peired AJ, Sisti A, Romagnani P. Mesenchymal Stem Cell-Based Therapy for Kidney Disease: A Review of Clinical Evidence. *Stem Cells Int.* 2016;2016:4798639.

10. Klinkhammer BM, Kramann R, Mallau M, et al. Mesenchymal stem cells from rats with chronic kidney disease exhibit premature senescence and loss of regenerative potential. *PLoS One.* 2014;9(3):e92115.

11. Yun SP, Yoon YM, Lee JH, et al. Tauroursodeoxycholic Acid Protects against the Effects of P-Cresol-Induced Reactive Oxygen Species via the Expression of Cellular Prion Protein. *Int J Mol Sci.* 2018;19(2).

12. Granata S, Zaza G, Simone S, et al. Mitochondrial dysregulation and oxidative stress in patients with chronic kidney disease. *BMC Genomics.* 2009;10:388.

13. Zaza G, Granata S, Masola V, et al. Downregulation of nuclear-encoded genes of oxidative metabolism in dialyzed chronic kidney disease patients. *PLoS One.* 2013;8(10):e77847.

14. Liu XB, Wang JA, Ogle ME, Wei L. Prolyl hydroxylase inhibitor dimethyloxalylglycine enhances mesenchymal stem cell survival. *J Cell Biochem.* 2009;106(5):903-911.

15. Noh H, Yu MR, Kim HJ, et al. Uremic toxin p-cresol induces Akt-pathway-selective insulin resistance in bone marrow-derived mesenchymal stem cells. *Stem Cells.* 2014;32(9):2443-2453.

16. Lee JH, Ryu JM, Han YS, et al. Fucoidan improves bioactivity and vasculogenic potential of mesenchymal stem cells in murine hind limb ischemia associated with chronic kidney disease. *J Mol Cell Cardiol.* 2016;97:169-179.

17. Maung SC, El Sara A, Chapman C, Cohen D, Cukor D. Sleep disorders and chronic kidney disease. *World J Nephrol.* 2016;5(3):224-232.

18. Crooke A, Huete-Toral F, Colligris B, Pintor J. The role and therapeutic potential of melatonin in age-related ocular diseases. *J Pineal Res.* 2017;63(2).

19. Mayo JC, Sainz RM, Gonzalez Menendez P, Cepas V, Tan DX, Reiter RJ. Melatonin and sirtuins: A "not-so unexpected" relationship. *J Pineal Res.* 2017;62(2).

20. Hardeland R. Melatonin and the pathologies of weakened or dysregulated circadian oscillators. *J Pineal Res.* 2017;62(1).

21. Lee SJ, Jung YH, Oh SY, Yun SP, Han HJ. Melatonin enhances the human mesenchymal stem cells motility via melatonin receptor 2 coupling with Galphaq in skin wound healing. *J Pineal Res.* 2014;57(4):393-407.

22. Yun SP, Han YS, Lee JH, Kim SM, Lee SH. Melatonin Rescues Mesenchymal Stem Cells from Senescence Induced by the Uremic Toxin p-Cresol via Inhibiting mTOR-Dependent Autophagy. *Biomol Ther (Seoul).* 2017.

23. Chang CL, Sung PH, Sun CK, et al. Protective effect of melatonin-supported adipose-derived mesenchymal stem cells against small bowel ischemia-reperfusion injury in rat. *J Pineal Res.* 2015;59(2):206-220.

24. Yip HK, Chang YC, Wallace CG, et al. Melatonin treatment improves adipose-derived mesenchymal stem cell therapy for acute lung ischemia-reperfusion injury. *J Pineal Res.* 2013;54(2):207-221.

25. Lee JH, Han YS, Lee SH. Potentiation of biological effects of mesenchymal stem cells in ischemic conditions by melatonin via upregulation of cellular prion protein expression. *J Pineal Res.* 2017;62(2).

26. Noh H, Yu MR, Kim HJ, et al. Uremia induces functional incompetence of bone marrow-derived stromal cells. *Nephrol Dial Transplant.* 2012;27(1):218-225.

27. Niiyama H, Huang NF, Rollins MD, Cooke JP. Murine model of hindlimb ischemia. *J Vis Exp.* 2009(23).

28. Rong Z, Wang M, Hu Z, et al. An effective approach to prevent immune rejection of human ESC-derived allografts. *Cell Stem Cell.* 2014;14(1):121-130.

29. Han YS, Kim SM, Lee JH, Lee SH. Co-Administration of Melatonin Effectively Enhances the Therapeutic Effects of Pioglitazone on Mesenchymal Stem Cells Undergoing Indoxyl Sulfate-Induced Senescence through Modulation of Cellular Prion Protein Expression. *Int J Mol Sci.* 2018;19(5).

30. Zhu P, Liu J, Shi J, et al. Melatonin protects ADSCs from ROS and enhances their therapeutic potency in a rat model of myocardial infarction. *J Cell Mol Med.* 2015;19(9):2232-2243.

31. Boilan E, Winant V, Dumortier E, et al. Role of Prion protein in premature senescence of human fibroblasts. *Mech Ageing Dev.* 2018;170:106-113.

32. Emamgholipour S, Hossein-Nezhad A, Sahraian MA, Askarisadr F, Ansari M. Evidence for possible role of melatonin in reducing oxidative stress in multiple sclerosis through its effect on SIRT1 and antioxidant enzymes. *Life Sci.* 2016;145:34-41.

33. Yu L, Gong B, Duan W, et al. Melatonin ameliorates myocardial ischemia/reperfusion injury in type 1 diabetic rats by preserving mitochondrial function: role of AMPK-PGC-1alpha-SIRT3 signaling. *Sci Rep.* 2017;7:41337.
34. Zhai M, Li B, Duan W, et al. Melatonin ameliorates myocardial ischemia reperfusion injury through SIRT3-dependent regulation of oxidative stress and apoptosis. *J Pineal Res.* 2017;63(2).
35. Chen D, Steele AD, Hutter G, et al. The role of calorie restriction and SIRT1 in prion-mediated neurodegeneration. *Exp Gerontol.* 2008;43(12):1086-1093.
36. Lisowski P, Kannan P, Mlody B, Prigione A. Mitochondria and the dynamic control of stem cell homeostasis. *EMBO Rep.* 2018;19(5).
37. Osellame LD, Blacker TS, Duchen MR. Cellular and molecular mechanisms of mitochondrial function. *Best Pract Res Clin Endocrinol Metab.* 2012;26(6):711-723.
38. Cui H, Kong Y, Zhang H. Oxidative stress, mitochondrial dysfunction, and aging. *J Signal Transduct.* 2012;2012:646354.
39. Lee S, Jeong SY, Lim WC, et al. Mitochondrial fission and fusion mediators, hFis1 and OPA1, modulate cellular senescence. *J Biol Chem.* 2007;282(31):22977-22983.
40. Kondapalli C, Kazlauskaite A, Zhang N, et al. PINK1 is activated by mitochondrial membrane potential depolarization and stimulates Parkin E3 ligase activity by phosphorylating Serine 65. *Open Biol.* 2012;2(5):120080.
41. Miele G, Jeffrey M, Turnbull D, Manson J, Clinton M. Ablation of cellular prion protein expression affects mitochondrial numbers and morphology. *Biochem Biophys Res Commun.* 2002;291(2):372-377.
42. Limbourg A, Korff T, Napp LC, Schaper W, Drexler H, Limbourg FP. Evaluation of postnatal arteriogenesis and angiogenesis in a mouse model of hind-limb ischemia. *Nat Protoc.* 2009;4(12):1737-1746.

43. Creager MA, Kaufman JA, Conte MS. Clinical practice. Acute limb ischemia. *N Engl J Med.* 2012;366(23):2198-2206.

44. Tebebi PA, Kim SJ, Williams RA, et al. Improving the therapeutic efficacy of mesenchymal stromal cells to restore perfusion in critical limb ischemia through pulsed focused ultrasound. *Sci Rep.* 2017;7:41550.

45. MacAskill MG, Saif J, Condie A, et al. Robust Revascularization in Models of Limb Ischemia Using a Clinically Translatable Human Stem Cell-Derived Endothelial Cell Product. *Mol Ther*. 2018;26(7):1669-1684.

FIGURE LEGENDS

FIGURE 1 Mesenchymal stem cells in chronic kidney disease (CKD-mMSCs) are susceptible to cell senescence by oxidative stress. (A) MSCs from normal or CKD mouse models treated with H_2O_2 (5–25 μM) for 72 h, and representative images of senescence-associated β-galactosidase (SA-β-gal) activity staining are shown. Scale bar = 100 μm; (B) Number of SA-β-gal positive cells (n = 3; biological replicates). The values represent the means ± standard error of the mean (SEM). **P* < 0.05 and ***P* < 0.01 vs. untreated, ##*P* < 0.01 vs. normal-mMSC group. (C) Normal and CKD-mMSCs treated with H_2O_2 (5–25 μM) for 72 h, and representative images for assessment of cellular morphology. Scale bar = 200 μm (D) Quantification of cell size. (n = 3; biological replicates). The values represent the means ± standard error of the mean (SEM). ***P* < 0.01 vs. untreated, ##*P* < 0.01 vs. normal-mMSC group. (E-H) Western blotting for p-P53 (E), p16INK4A (F), SMP30 (G), and p21 (H) in normal and CKD-mMSCs treated with H_2O_2 (5–25 μM) for 72 h (n = 3; biological replicates). The values represent the means ± standard error of the mean (SEM). ***P* < 0.01 vs. untreated, ##*P* < 0.01 vs. normal-mMSC group.

FIGURE 2 Melatonin inhibits oxidative stress-induced cell senescence in mesenchymal stem cells in chronic kidney disease (CKD-mMSCs). (A) Cell morphology. Representative image of H_2O_2 (25 μM, for 72 h)-exposed normal and CKD-mMSCs pretreated with melatonin (1 nM–100 μM). (B) Quantification of cell size. (n = 3; biological replicates). The values represent the means ± standard error of the mean (SEM). ***P* < 0.01 vs. untreated, ##*P* < 0.01 vs. H_2O_2, $$*P* < 0.01 vs. normal-mMSC group. (C) SA-β-gal activity stain assay. Representative image of H_2O_2 (25 μM, for 72 h)-exposed normal and CKD-mMSCs pretreated with melatonin (1 nM–100 μM). Scale bar = 100 μm. (D) Number of SA-β-gal positive cells (n = 3; biological replicates). The values represent the means ± standard error of the mean (SEM). ***P* < 0.01 vs. untreated, ##*P* < 0.01 vs. H_2O_2, $$*P* < 0.01 vs. normal-mMSC group. (E-H) Western blotting for p-P53 (E), p16INK4A (F), SMP30 (G), and p21 (H) in H_2O_2 (25 μM, for 72 h)-exposed normal and CKD-mMSCs pretreated with melatonin (1 nM–100 μM) (n = 3; biological replicates). The values represent the means ± standard error of the mean (SEM). ***P* < 0.01 vs. untreated, ##*P* < 0.01 vs. H_2O_2, $$*P* < 0.01 vs. normal-mMSC group.

FIGURE 3 Melatonin protects against oxidative stress-induced cell senescence via PrP^C. (A) Western blotting for PrP^C in H_2O_2 (25 μM, for 72 h)-exposed normal and mesenchymal stem cells in chronic kidney disease (CKD-mMSCs) pretreated with melatonin (100 μM) (n = 3; biological replicates). The values represent the means ± standard error of the mean (SEM). ***P* < 0.01 vs. untreated, ##*P* < 0.01 vs. H_2O_2, $$*P* < 0.01 vs. normal-mMSC group. (B-E) Western blotting for p-P53 (B), p16INK4A (C), SMP30 (D), and p21 (E) in H_2O_2 (25 μM, for 72 h)-exposed *PRNP* siRNA transfected CKD-mMSCs pretreated with melatonin (100 μM) (n = 3; biological replicates). The values represent the means ± standard error of the mean

(SEM). *P < 0.05 and **P < 0.01 vs. normal-mMSC, ##P < 0.01 vs. CKD-mMSC, $$$P$ < 0.01 vs. H_2O_2 + CKD-mMSC, &&P < 0.01 vs. H_2O_2 + Melatonin + *siPRNP*-CKD-mMSC. (F-I) Western blotting for p-P53 (F), p16INK4A (G), SMP30 (H), and p21 (I) in H_2O_2 (25 μM, for 72 h)-exposed PRNP siRNA transfected normal-mMSCs (n = 3; biological replicates). The values represent the means ± standard error of the mean (SEM). *P < 0.05 and **P < 0.01 vs. untreated, ##P < 0.01 vs. H_2O_2, $$$P$ < 0.01 vs. H_2O_2 + *siPRNP*. (J) SA-β-gal activity stain assay. Representative image of H_2O_2 (25 μM, for 72 h)-exposed *PRNP* siRNA transfected normal-mMSCs. Scale bar = 100 μm. (K) Number of SA-β-gal positive cells (n = 3; biological replicates). The values represent the means ± standard error of the mean (SEM). **P < 0.01 vs. untreated, ##P < 0.01 vs. H_2O_2, $$$P$ < 0.01 vs. H_2O_2 + *siPRNP*.

FIGURE 4 Melatonin protects mitochondrial function in mesenchymal stem cells in chronic kidney disease (CKD-mMSCs). (A) PINK1 bound to PrP^C in H_2O_2 (25 μM, for 72 h)-exposed *PRNP* siRNA transfected CKD-mMSCs pretreated with melatonin (100 μM), which was confirmed via co-immunoprecipitation (co-IP) (n = 3; biological replicates). The values represent the means ± standard error of the mean (SEM). *P < 0.05 and **P < 0.01 vs. normal-mMSC, ##P < 0.01 vs. CKD-mMSC, $$$P$ < 0.01 vs. Melatonin + *siPRNP*. (B-E) Western blotting for PINK1, pS637-DRP-1, Mfn-1, and OPA-1 in H_2O_2 (25 μM, for 72 h)-exposed *PRNP* siRNA transfected CKD-mMSCs pretreated with melatonin (100 μM) (n = 3; biological replicates). The values represent the means ± standard error of the mean (SEM). *P < 0.01 and **P < 0.01 vs. normal-mMSC, ##P < 0.01 vs. CKD-mMSC, $$$P$ < 0.01 vs. H_2O_2 + CKD-mMSC, &&P < 0.01 vs. H_2O_2 + Melatonin + *siPRNP* -CKD-mMSC. (F) Mitochondrial morphology was evaluated by Mito-Tracker Red staining. Confocal imaging of mitochondria undergoing fusion or fission in normal mMSCs or CKD cells (n = 3; biological replicates). Scale bar = 10 μm. (G, H) Complex I and IV enzyme activity assay in

H_2O_2 (25 μM, for 72 h)-exposed *PRNP* siRNA transfected CKD-mMSCs pretreated with melatonin (100 μM) (n = 3; biological replicates). The values represent the means ± standard error of the mean (SEM). **P* < 0.05 and ***P* < 0.01 vs. normal-mMSC, ##*P* < 0.01 vs. CKD-mMSC, $$*P* < 0.01 vs. H_2O_2 + CKD-mMSC, &&*P* < 0.01 vs. H_2O_2 + Melatonin + *siPRNP*-CKD-mMSC. (I) Oxygen consumption ratio in normal and CKD-mMSCs (n = 3; biological replicates). The values represent the means ± standard error of the mean (SEM). ***P* < 0.01.

FIGURE 5 Melatonin restores the biological activity of mesenchymal stem cells in chronic kidney disease (CKD-mMSCs) via increased PrP^C expression. (A and B) Western blotting for CKD2, Cyclin E, CKD4, and Cyclin D1 in H_2O_2 (25 μM, for 72 h)-exposed *PRNP* siRNA transfected CKD-mMSCs pretreated with melatonin (100 μM) (n = 3; biological replicates). The values represent the means ± standard error of the mean (SEM). ***P* < 0.01 vs. normal-mMSC, ##*P* < 0.01 vs. CKD-mMSC, $$*P* < 0.01 vs. H_2O_2 + CKD-mMSC, &&*P* < 0.01 vs. H_2O_2 + Melatonin + *siPRNP*-CKD-mMSC. (C, D) Carboxyfluorescein succinimidyl ester (CFSE)-labeled H_2O_2 (25 μM, for 72 h)-exposed *PRNP* siRNA transfected CKD-mMSCs pretreated with melatonin (100 μM); cell proliferation was assessed by fluorescence-activated cell sorting (FACS) analysis of the dilution of CFSE in the same number of viable cells (n = 3; biological replicates). The values represent the means ± standard error of the mean (SEM). ***P* < 0.01 vs. normal-mMSC, ##*P* < 0.01 vs. CKD-mMSC, $$*P* < 0.01 vs. H_2O_2 + CKD-mMSC, &&*P* < 0.01 vs. H_2O_2 + Melatonin + *siPRNP* -CKD-mMSC. (E) The S phase of the cells was evaluated by flow cytometry using propidium iodide (PI) staining. (F) Quantification of the percentage of cells in S phase. The values represent the means ± standard error of the mean (SEM). ***P* < 0.01 vs. normal-mMSC, ##*P* < 0.01 vs. CKD-mMSC, $$*P* < 0.01 vs. H_2O_2 + CKD-mMSC, &&*P* < 0.01 vs. H_2O_2 + Melatonin + *siPRNP*-CKD-mMSC. (G) Single-cell cultures of H_2O_2 (25 μM, for 72 h)-exposed *PRNP* siRNA

transfected CKD-mMSCs pretreated with melatonin (100 μM) were stained with Giemsa after 10 d of culturing. Scale bar = 100 μm; (H) images of the number of cells per well in 96-well plates (n = 3; biological replicates). The values represent the means ± standard error of the mean (SEM). ***P* < 0.01 vs. untreated, ##*P* < 0.01 vs. H_2O_2, $$*P* < 0.01 vs. H_2O_2 + Melatonin + *siPRNP*, &&*P* < 0.01 vs. Normal-mMSC group. (I) Adhesion assay of H_2O_2 (25 μM, for 72 h)-exposed *PRNP* siRNA transfected CKD-mMSCs pretreated with melatonin (100 μM) were stained with Crystal Violet after 1 hour of cell incubation and attachment. Scale bar = 100 μm; (J) Measurement of extracted stain solution from cells, OD 560 nm (n = 3; biological replicates). The values represent the means ± standard error of the mean (SEM). ***P* < 0.01 vs. Normal-mMSC, ##*P* < 0.01 vs. CKD-mMSC, $$*P* < 0.01 vs. H_2O_2 + CKD-mMSC, &&*P* < 0.01 vs. H_2O_2 + Melatonin + *siPRNP*-CKD-mMSC. (K) ELISA for vascular endothelial growth factor (VEGF), fibroblast growth factor (FGF), and hepatocyte growth factor (HGF) levels in H_2O_2 (25 μM, for 72 h)-exposed *PRNP* siRNA transfected CKD-mMSCs pretreated with melatonin (100 μM) (n = 3; biological replicates). The values represent the means ± standard error of the mean (SEM). **P* < 0.05 and ***P* < 0.01 vs. Normal-mMSC, ##*P* < 0.01 vs. CKD-mMSC, $$*P* < 0.01 vs. H_2O_2 + CKD-mMSC, &&*P* < 0.01 vs. H_2O_2 + Melatonin + *siPRNP*-CKD-mMSC.

FIGURE 6 Melatonin increases the survival of transplanted mesenchymal stem cells in chronic kidney disease (CKD-mMSCs) via PrP^C expression.

(A and B) ELISA for IL-10 and TNF-α expression levels in ischemic limb tissues on postoperative day 3. The values represent the means ± standard error of the mean (SEM). ***P* < 0.01 vs. PBS, ##*P* < 0.01 vs. Normal-mMSC, $$*P* < 0.01 vs. CKD-mMSC, &&*P* < 0.01 vs. Melatonin + *siPRNP*-CKD-mMSC. (C and D) Immunofluorescence staining for IL-10 and TNF-α in ischemic limb tissues on day 3 after ischemia (n = 5; biological replicates).

Scale bar = 50 μm. (E and F) Immunofluorescence staining for cleaved caspase-3 (Caspase-3; red) and GFP (labeled for MSCs; green) in ischemic limb tissues on day 3 after ischemia (n = 5; biological replicates). Scale bar = 50 μm. Arrows indicate double positive cells. Apoptosis of transplanted MSCs was assessed via cleaved caspase-3 and GFP double-positive cells. The values represent the means ± standard error of the mean (SEM). N.D, No detection, $^{**}P < 0.01$ vs. Normal mMSC, $^{\#\#}P < 0.01$ vs. CKD-mMSC, $^{\$\$}P < 0.01$ vs. CKD-mMSC + Melatonin, $^{\&\&}P < 0.01$ vs. *siPRNP* + CKD-mMSC + Melatonin. (G and H) TUNEL staining in ischemic limb tissues on day 3 after ischemia (n = 5; biological replicates). Scale bar = 50 μm. The values represent the means ± standard error of the mean (SEM). $^{**}P < 0.01$ vs. PBS, $^{\#\#}P < 0.01$ vs. Normal-mMSC, $^{\$\$}P < 0.01$ vs. CKD-mMSC, $^{\&\&}P < 0.01$ vs. *siPRNP* + CKD-mMSC + Melatonin. (I and J) Immunofluorescence staining for Ki67 (red) and GFP (labeled for MSCs; green) in ischemic limb tissues in ischemic limb tissues on day 3 after ischemia (n = 5; biological replicates). Scale bar = 50 μm. Arrows indicate double positive cells. Proliferation of transplanted MSCs was assessed on the basis of Ki67 and GFP double-positive cells. The values represent the means ± standard error of the mean (SEM). N.D, No detection, $^{**}P < 0.01$ vs. Normal mMSC, $^{\#\#}P < 0.01$ vs. CKD-mMSC, $^{\$\$}P < 0.01$ vs. CKD-mMSC + Melatonin, $^{\&\&}P < 0.01$ vs. *siPRNP* + CKD-mMSC + Melatonin. (K and L) Immunofluorescence staining for PCNA (red) and GFP (labeled for MSCs; green) in ischemic limb tissues in ischemic limb tissues on day 3 after ischemia (n = 5; biological replicates). Scale bar = 50 μm. Arrows indicate double positive cells. Proliferation of transplanted MSCs was assessed via the PCNA and GFP double-positive cells. The values represent the means ± standard error of the mean (SEM). N.D, No detection, $^{**}P < 0.01$ vs. Normal mMSC, $^{\#\#}P < 0.01$ vs. CKD-mMSC, $^{\$\$}P < 0.01$ vs. CKD-mMSC + Melatonin, $^{\&\&}P < 0.01$ vs. *siPRNP* + CKD-mMSC + Melatonin.

FIGURE 7 Assessment of functional recovery by mesenchymal stem cell (MSC) transplantation in a murine hind limb ischemia model.

(A) ELISA for vascular endothelial growth factor (VEGF), fibroblast growth factor (FGF), and hepatocyte growth factor (HGF) levels in ischemic sites of mice injected after 3 d with PBS, Normal-mMSCs, CKD-mMSCs, CKD-mMSCs with melatonin, *PRNP* siRNA transfected CKD-mMSCs with melatonin, and Scramble siRNA transfected CKD-mMSCs with melatonin. The values represent the means ± standard error of the mean (SEM). **P* < 0.05 and ***P* < 0.01 vs. PBS, $^{\#\#}P$ < 0.01 vs. Normal mMSC, $^{\$\$}P$ < 0.01 vs. CKD-mMSC, $^{\&\&}P$ < 0.01 vs. *siPRNP* + CKD-mMSC + Melatonin. (B) Laser Doppler imaging-based evaluation of the blood flow recovery in ischemic sites of mice injected with PBS, Normal-mMSCs, CKD-mMSCs, CKD-mMSCs with melatonin, *PRNP* siRNA transfected CKD-mMSCs with melatonin, and Scramble siRNA transfected CKD-mMSCs with melatonin. Blood flow was measured on days 0, 3, 7, 14, 21, and 28 (n = 5; biological replicates). (C) The ratio of blood perfusion (blood flow in the left ischemic limb/blood flow in the right non-ischemic limb) was measured in each group. The values represent the means ± standard error of the mean (SEM). ***P* < 0.01 vs. PBS, ##*P* < 0.01 vs. Normal-mMSC, $$*P* < 0.01 vs. CKD-mMSC. (D) Representative image illustrating the various outcomes (foot necrosis, toe loss, and limb salvage) of mouse ischemic limbs on postoperative day 28, and distribution of the different outcomes on postoperative day 28 in each group (n = 5; biological replicates). (E) The capillary density in ischemic tissues was evaluated 28 d after MSC transplantation, via CD31 immunostaining. Scale bar = 50 μm. (F) Capillary density was quantified as the CD31-positive/mm^2. The values represent the means ± standard error of the mean (SEM). ***P* < 0.01 vs. PBS, ##*P* < 0.01 vs. Normal-mMSC, $$*P* < 0.01 vs. CKD-mMSC, &&*P* < 0.01 vs. Melatonin + *siPRNP*-CKD-mMSC. (G) Arteriole density in ischemic tissues was evaluated 28 d after MSC transplantation, using αSMA immunostaining. Scale bar = 50 μm.

(H) Arterioles density was quantified as the number of α-SMA-positive/mm^2. The values represent the means ± standard error of the mean (SEM). ***P* < 0.01 vs. PBS, ##*P* < 0.01 vs. Normal-mMSC, $$*P* < 0.01 vs. CKD-mMSC, &*P* < 0.05 and &&*P* < 0.01 vs. Melatonin + *siPRNP*-CKD-mMSC. (I) Hematoxylin and eosin staining to evaluate tissue necrosis in the ischemic hind limb (n = 5; biological replicates). Scale bar =100 μm. (J) Necrosis area was quantified as the percentage of necrosis. The values represent the means ± standard error of the mean (SEM). ***P* < 0.01 vs. PBS, ##*P* < 0.01 vs. Nor-mMSC, $$*P* < 0.01 vs. CKD-mMSC, &&*P* < 0.01 vs. *siPRNP* + CKD-mMSC + Mela. (K) Sirius red staining to evaluate collagen fibers in the ischemic hind limb (n = 5; biological replicates). Scale bar =100 μm. (L) Collagen fibrosis area was quantified as the percentage of Sirius red-stained area. The values represent the means ± standard error of the mean (SEM). ***P* < 0.01 vs. PBS, ##*P* < 0.01 vs. Nor-mMSC, $$*P* < 0.01 vs. CKD-mMSC, &&*P* < 0.01 vs. *siPRNP* + CKD-mMSC + Mela.

FIGURE 8 A schematic representation of the proposed mechanism by which melatonin inhibits mitochondrial fusion of mesenchymal stem cells in chronic kidney disease (CKD-mMSCs) through regulation of PrP^C, thereby inhibiting senescence. Melatonin upregulates PrP^C in CKD-mMSCs. PrP^C upregulates PINK1, induces mitochondrial fission, and increases mitochondrial activity. Mitochondrial functional activity inhibits senescence in CKD-mMSCs, and restores cell function by increasing proliferation. Melatonin treatment of CKD-mMSCs increases survival in ischemic disease and improves neovascularization.

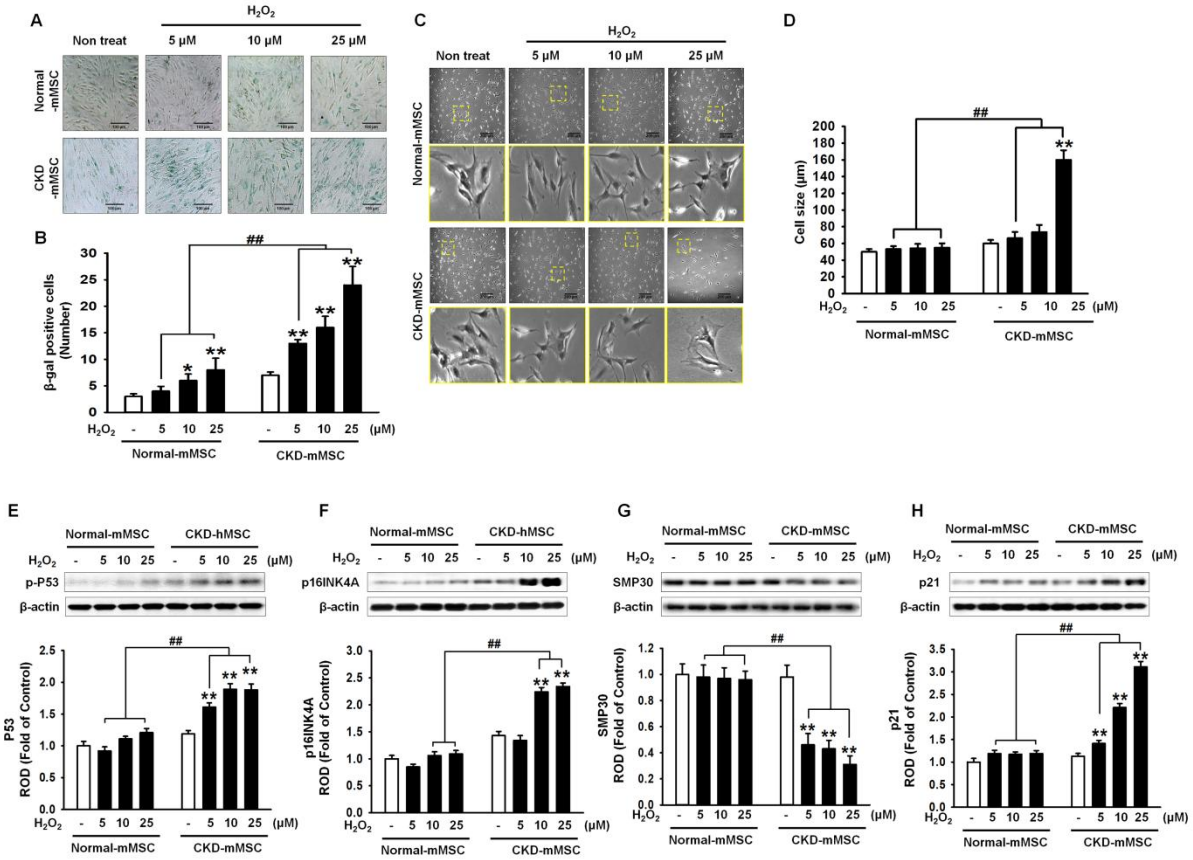

Figure.1

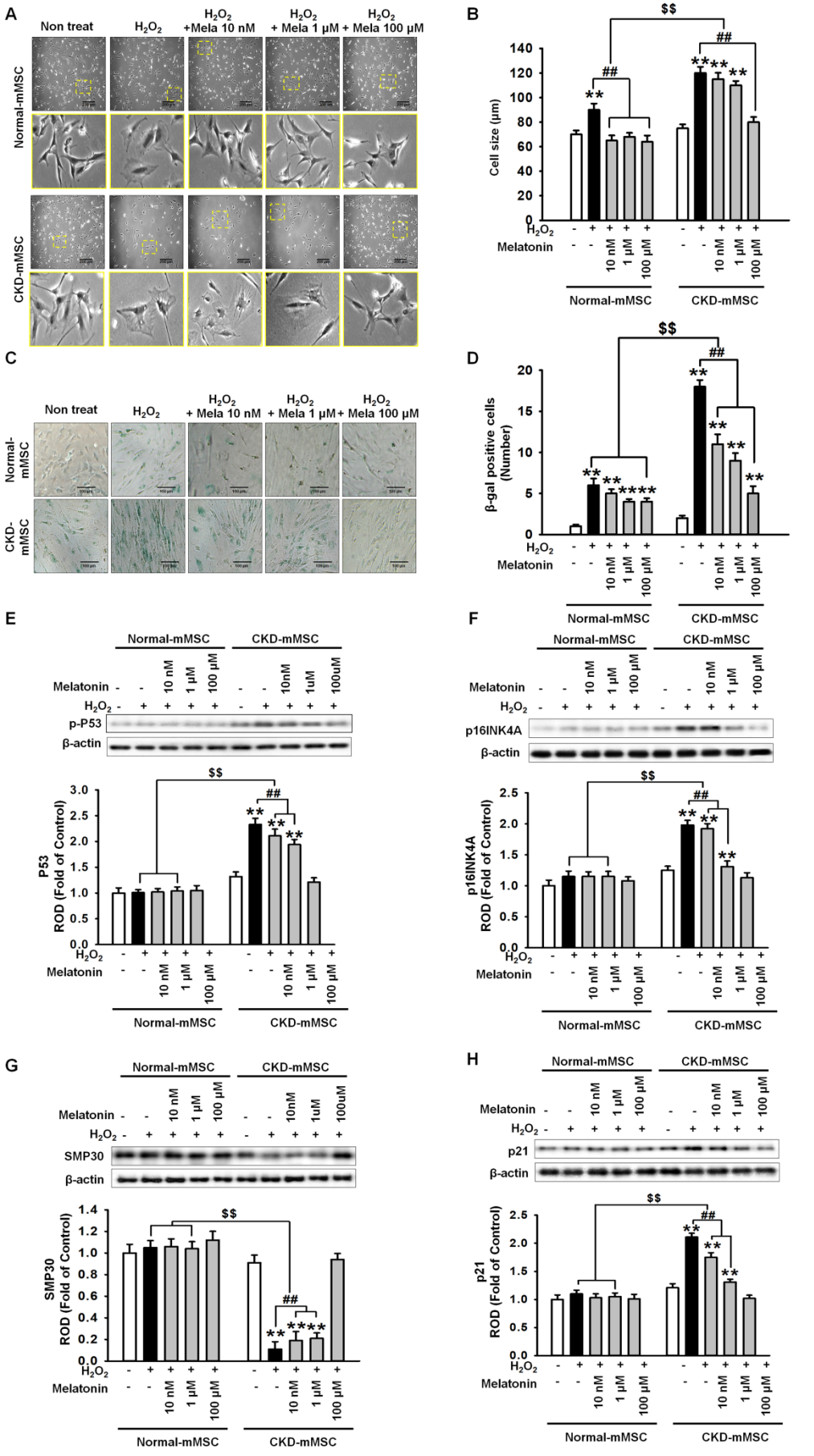

Figure.2

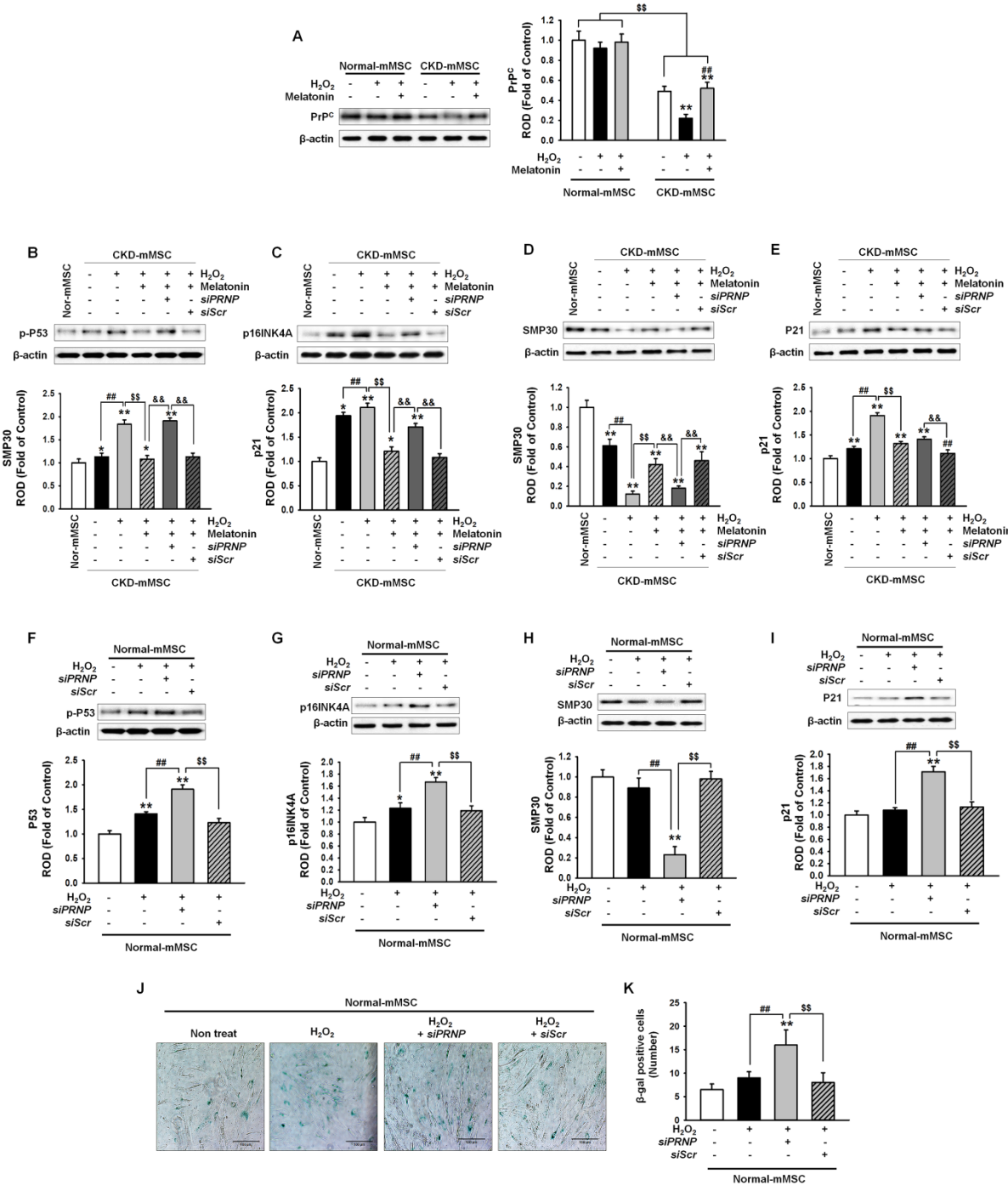

Figure.3

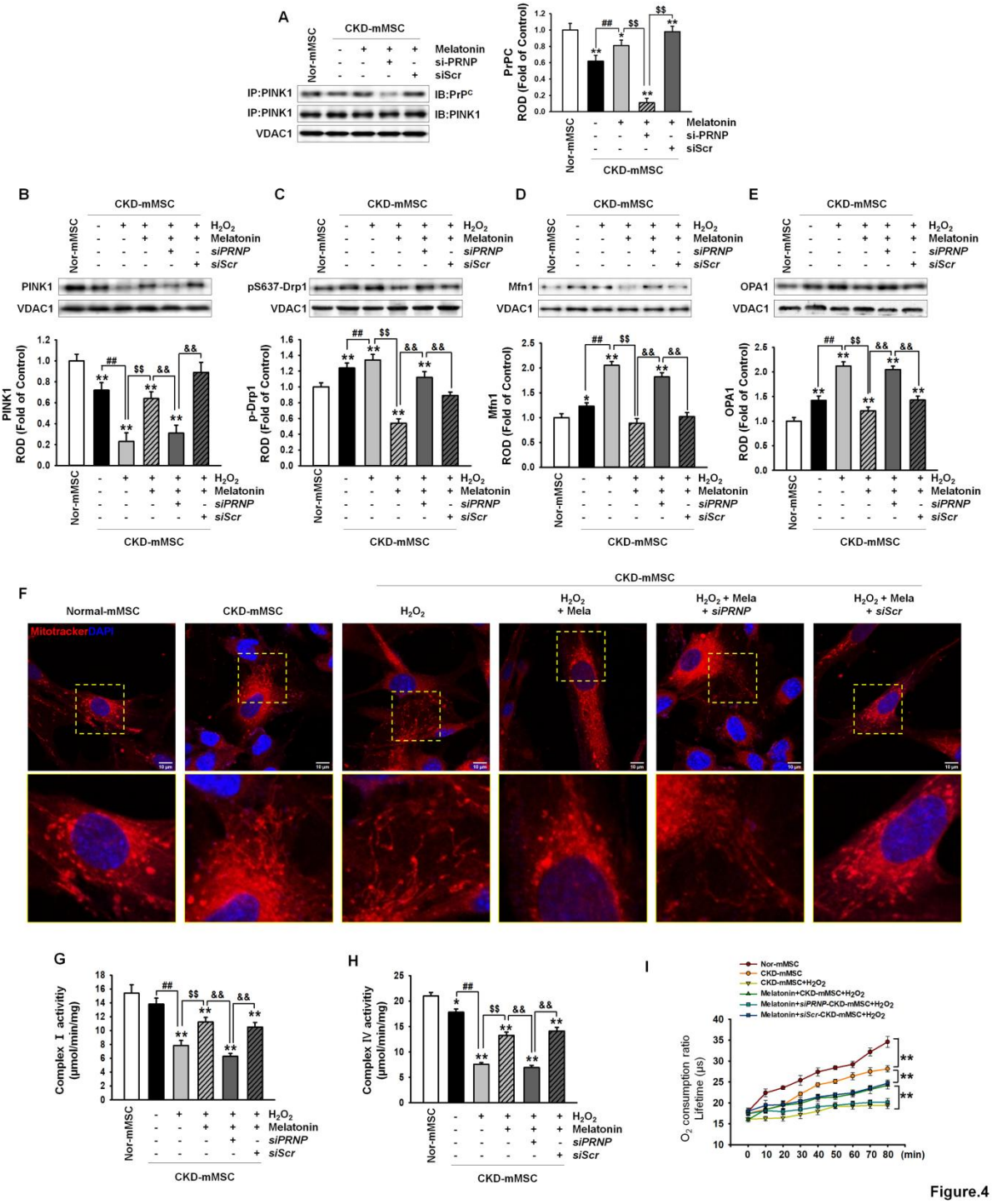

Figure.4

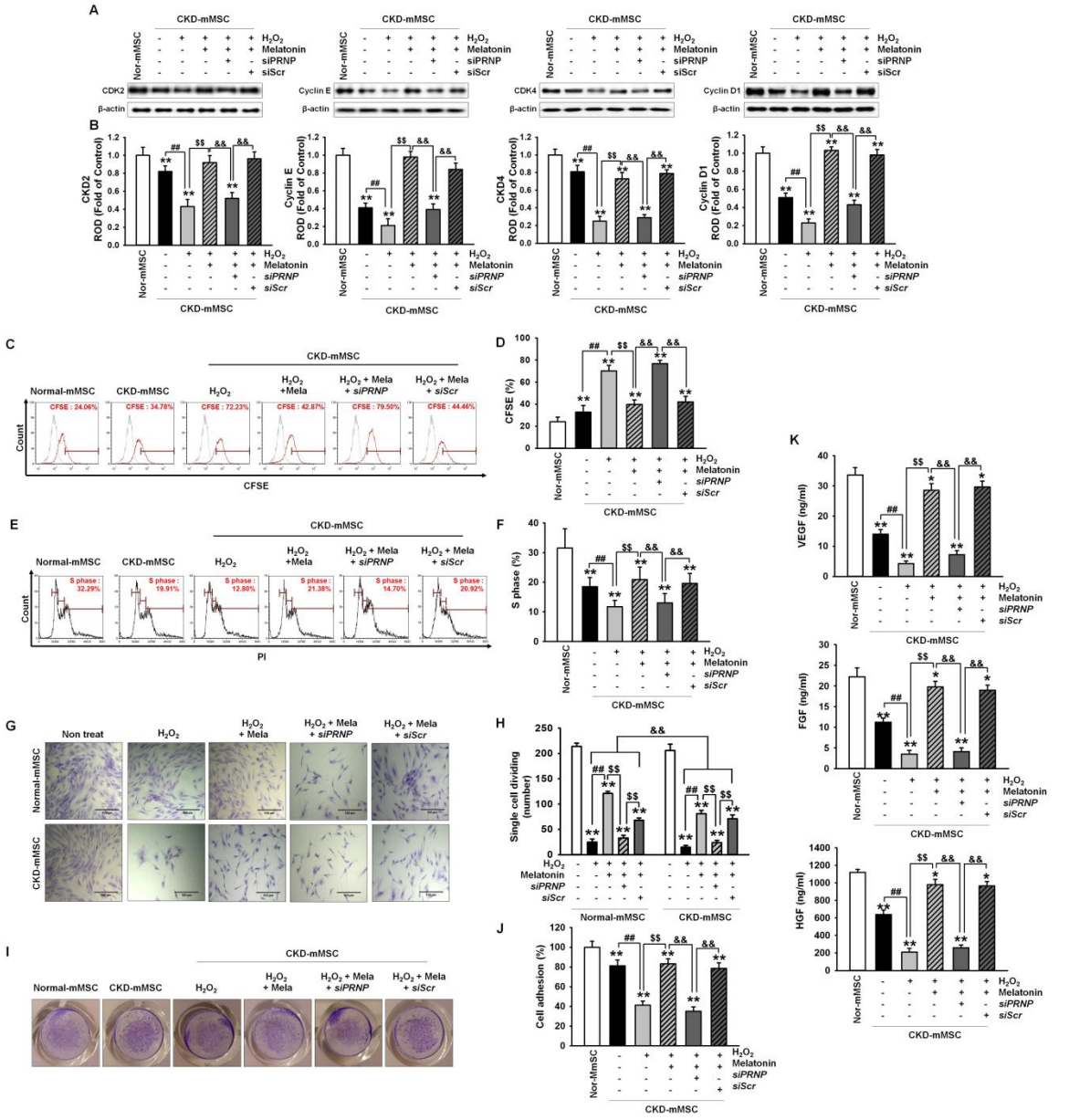

Figure.5

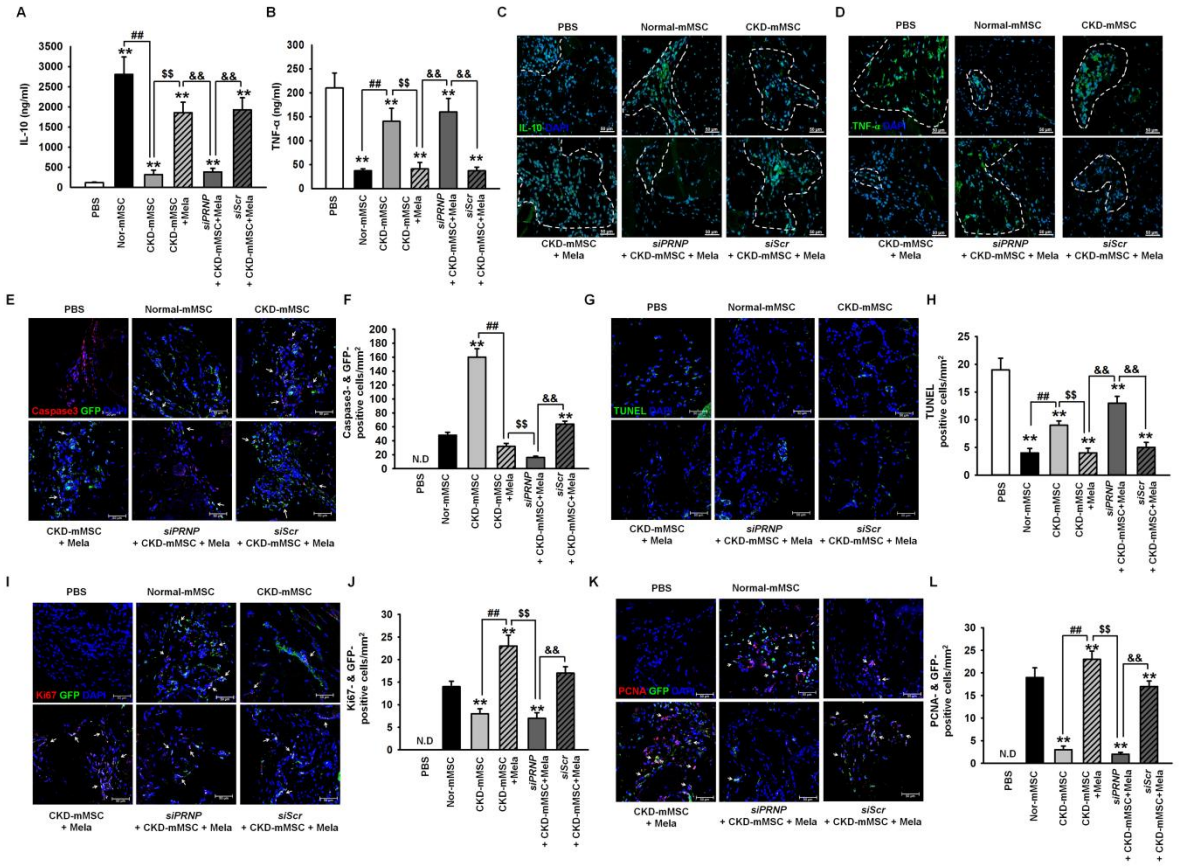

Figure.6

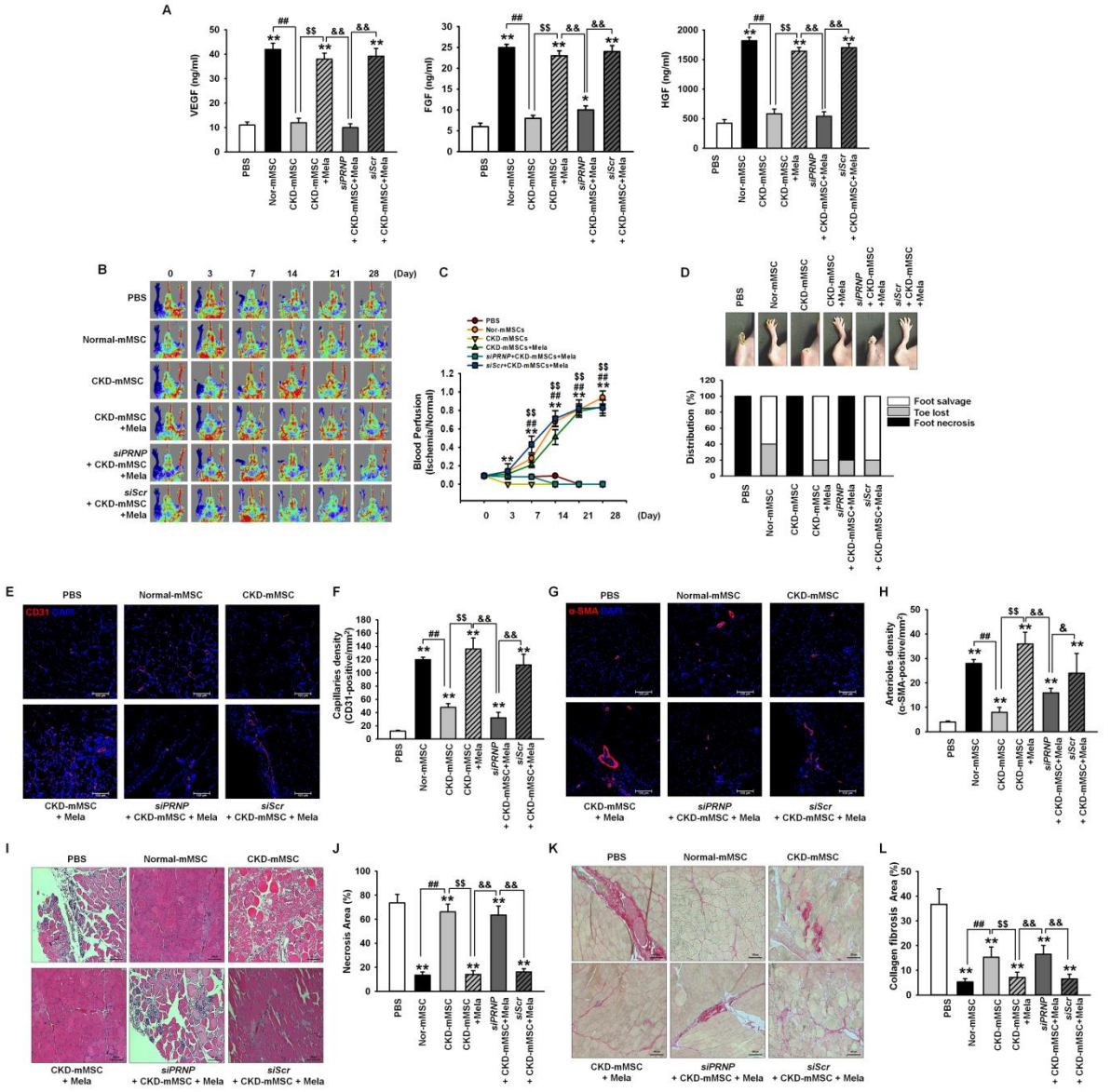

Figure.7

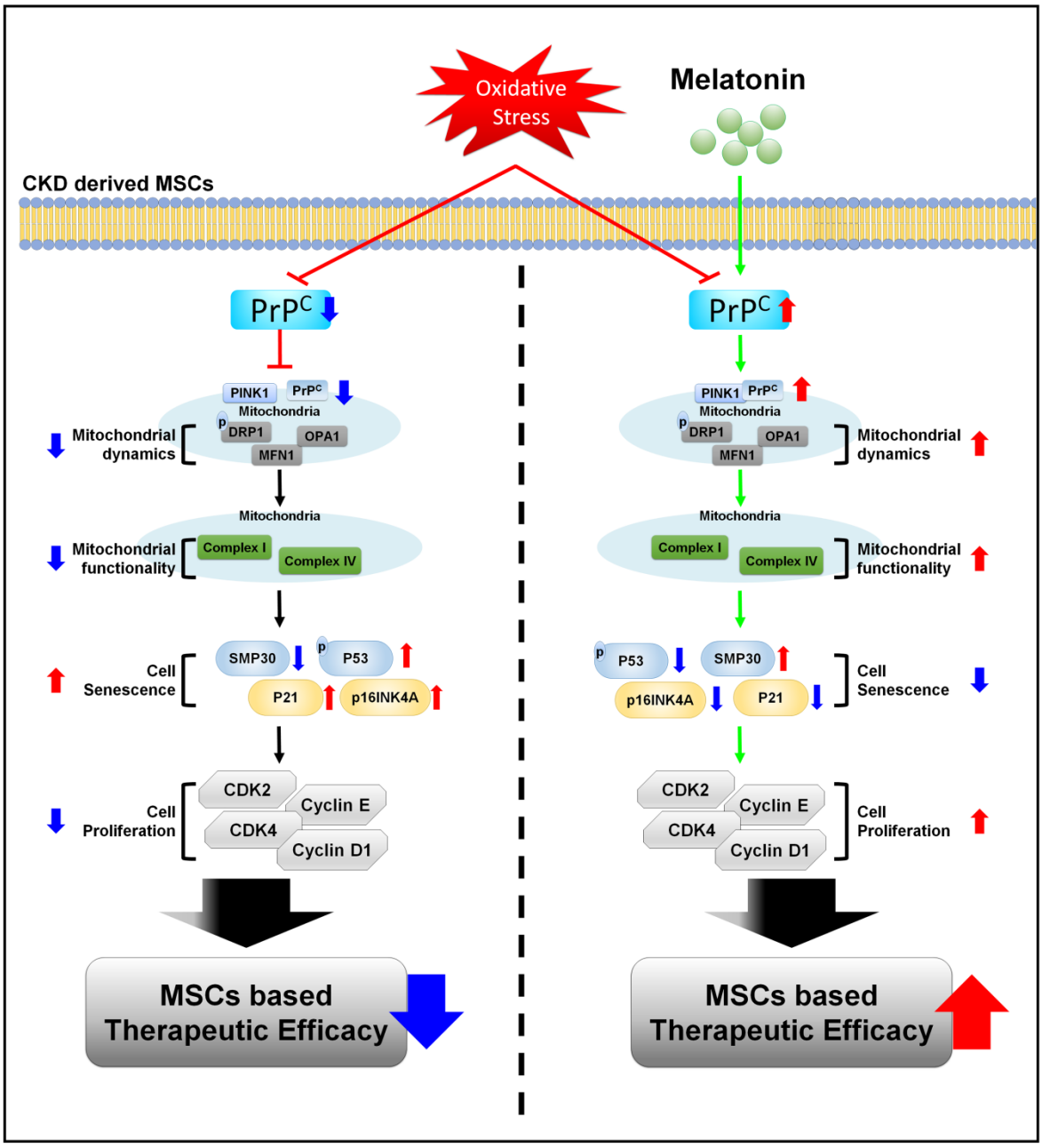

Figure.8